A Model of Granular Tribocharging for Dielectric Mixtures with Continuous Size Distributions

Dylan Carter and Christine Hartzell
Dept. of Aerospace Engineering
University of Maryland at College Park
phone: (1) 301-538-8923
e-mail: d.p.carter4@gmail.com

***Abstract*—Triboelectric charging, the phenomenon by which electrical charge accumulates during contact between two surfaces, has been known to cause significant charge separation in granular mixtures, even between chemically identical grains. This charging is a stochastic size-dependent process resulting from random collisions between grains. The prevailing models and experimental results suggest that, in most cases larger grains in a mixture acquire a positive charge, while smaller grains charge negatively. These models, and the experiments that use them, are typically restricted to mixtures of two discrete grain sizes, which are not representative of most naturally-occurring granular mixtures. We have developed a new model that predicts the average charge distribution in a granular mixture of any continuous size distribution. Expanding to continuous size distributions enables the prediction of charge separation in many natural granular phenomena, including terrestrial dust storms and mass wasting on the Moon and Mars. Furthermore, the expanded model makes new predictions about the charge distribution, including specific conditions under which the usual size-dependent polarity is reversed. We will also discuss experiments that are planned to test the grain charging predicted by our model.**

I. Introduction

Granular mixtures are susceptible to the generation of large electrical potential differences due to triboelectric charging, even when all grains are composed of the same material. This phenomenon is connected to the large electrical fields that often develop in sand storms [1-3] and ash clouds [4], and causes clumping and even dust explosions in powder-handling industries [5-8]. This type of charge exchange is stochastic due to the chemical symmetry among all grains, but trends can be observed in the charging behavior. Most experiments and rudimentary models for charge exchange predict that larger grains will tend to acquire a positive charge and smaller grains will become negatively charged, on average, with the degree of charge separation influenced primarily by the size differences and mass fractions of each discrete grain size [9-13]. Existing models for

this phenomenon neglect a number of important effects, and typically underestimate the magnitude of the charge exchange [13-14].

Based on earlier work by Lowell and Truscott [15-16], Lacks and Levandovsky developed an analytical model for predicting average grain charge separation due to the transfer of trapped high-energy electrons during random grain collisions [13]. In this paper, we expand their model of tribocharging to make predictions about the charge distribution in mixtures with a continuous size distribution and include originally neglected effects. Although the experimental evidence for Lacks and Levandovsky's original model is promising, the model itself is strikingly simplistic. In their initial discussion, they note that they have ignored a variety of phenomena, including the effect of aspherical shapes, sliding contact, and electrostatic forces between grains, which may alter the charge exchange rate [13]. The resulting model describes individual charge exchange events as identical for all pairs of grains regardless of grain size [11-14]. Because the magnitude of insulator tribocharging is shown to be highly dependent on the area in contact [15-21], we introduce an additional term A_{ij}, the contact area between grains of radii R_i and R_j during a collision. This causes the amount of transferred charge during a collision to depend upon the relative sizes of the grains in contact, changing the properties of the charge distribution and making new predictions about charging trends for various size distributions.

II. Theory

A. Assumptions and definitions

1) Transfer mechanism

For the purposes of this model, we will adopt the model for charge transfer proposed by Lowell and Truscott [15-16] and further elaborated by Lacks and Levandovsky [12-13] (see Fig. 1). Each grain is assumed to be a solid sphere of radius R; its surface area is therefore $4\pi R^2$. The surface area density of trapped high-energy electrons is ρ_H and is initially the same for all grains. Its value at time $t = 0$ (before charge exchange due to mixing) is given by ρ_0, at which time all grains are electrically neutral. According to the trapped electron model, each collision exposes some number of high-energy electrons that each have a random probability of being transferred; we will denote this probability as f_H. In addition, we will assume that each collision involves some characteristic contact area A_{ij}, where the colliding grains have radii R_i and R_j. We will further assume that the relative speed between grains is size-independent and equal for all grains, and that they are all composed of the same material; therefore, the contact area is a function of the grains' radii only. This allows us to express the number of high-energy electrons transferred from a grain of radius R_i to a grain of radius R_j as $f_H \rho_{Hi} A_{ij}$. Note that the average surface density of high-energy electrons ρ_H is a function of time, and therefore varies throughout the mixing process.

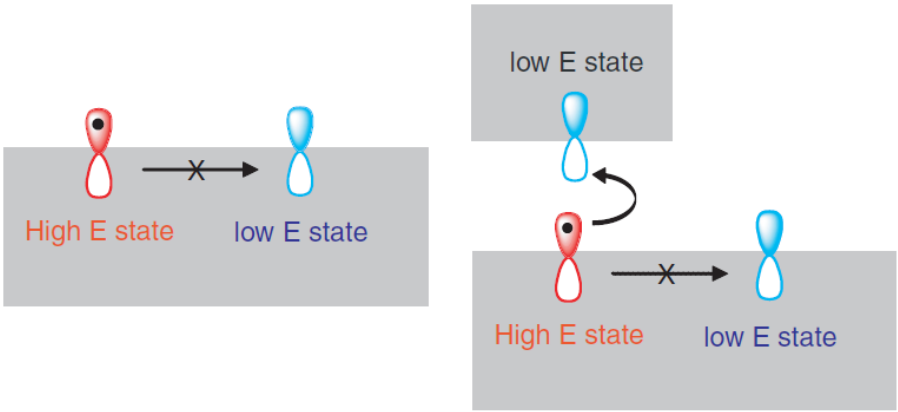

(a) (b)

Fig. 1. Process of electron transfer during insulator contact (from Lacks and Levandovsky, 2006 [13]). (a) Surface electrons can be trapped in high-energy states, unable to transition to low-energy states due to localization of electrons. (b) During collisions, low-energy states on another surface can be brought close enough to allow the electron to transfer to the other surface.

2) Particle size distribution (PSD)

Previous tribocharging models have been developed specifically for application to size distributions consisting of two discrete sizes [9, 13-14]. These models are restrictive, as granular mixtures in nature are much more accurately represented by continuous size distribution functions. While bi-disperse mixtures are much easier to manipulate analytically and are relevant to simple tribocharging experiments, they cannot explain or predict phenomena in natural granular mixtures. Thus, we will consider charge exchange in an arbitrary continuous grain size distribution.

Consider a mixture of grains with a size distribution of radii given by $g(R)$; that is, the fraction of grains in the mixture with a radius within dR of R is $g(R)$. The distribution is normalized to one over the space of all grain radii. As a result, the number of grains with radius R_j (here defined as n_j) is equal to $n_0\, g(R)\, dR$, where n_0 is the total number of grains in the mixture.

3) Collision rates

As in Lacks and Levandovsky's model, we assume that all grains move at approximately the same speed, and therefore that the average relative speed between two grains is a constant, here called v_r. We can use the relative speed between grains to estimate the collision rates as grains move through the mixture. Consider a single grain of radius R_i moving against a background of grains of radius R_j. The first grain moves with speed v_r relative to the background grains. In some time Δt, the grain moves a distance $v_r\, \Delta t$. In this time, it collides with any grains whose centers are a distance $R_i + R_j$ from the axis of its motion. Therefore, the moving grain collides with any grains within the volume $\pi\, (R_i + R_j)^2\, v_r\, \Delta t$. If our control volume is V_c and there are n_j grains with radius R_j in the mixture, then the rate at which our grain of radius R_i collides with grains of radius R_j is ω_{ij}, where:

$$\omega_{ij} = \pi \frac{v_r n_0 g(R_j)}{V_c} (R_i + R_j)^2 dR_j \quad (1)$$

4) Collision area

In experiments on rubbing flat surfaces together, the exchanged charge is directly proportional to the area exposed to contact, and collisions between small grains often involve both sliding contact as well as rebounding from a point contact [18-20]. From this observation, we may conclude that the exchange of charge in real collisions between grains will be heavily dependent on the surface area of the grains.

The inclusion of a collision area term is a stark departure from the typical approach used in previous granular tribocharging models. The model developed by Lacks and Levandovsky, and frequently employed to make predictions in various tribocharging experiments, assumes that a constant number of electrons is transferred during each collision [12-13]. This is analogous to the assertion that $f_H\ \rho_{Hi}(t)\ A_{ij}$ = constant. While this appears to create problems due to the fact that ρ_{Hi}(t) is time-dependent, we will later discover that this term divides out when calculating grain charge. Therefore, in calculating the final charge on the grains, the result is identical to the assumption that A_{ij} is a constant.

In Gugan's treatment [22] of Hertz's theory on contact area in collision between spheres, the collision area is given in terms of the collision speed U, reduced radius R^*, reduced mass M^*, and effective elastic coefficient X^*:

$$R^* = \frac{R_i R_j}{R_i + R_j} \quad (2)$$

$$M^* = \frac{m_i m_j}{m_i + m_j} \quad (3)$$

$$X^* = \frac{1-\nu_i^2}{E_i} + \frac{1-\nu_j^2}{E_j} \quad (4)$$

Because we are here assuming that all grains are of the same material, they all have the same density, modulus E, and Poisson's ratio ν. We have also assumed that the relative speed between any two grains is $v_r = U$ = constant, so all factors involving only these terms can be collected into a size-independent coefficient k_A:

$$A_{ij} = \left[16.4 U^2 X^* M^* (R_*)^2\right]^{2/5} = k_A r_{ij} R_i R_j \quad (5)$$

$$r_{ij} = \frac{R_i R_j}{\left(R_i^3 + R_j^3\right)^{2/5} \left(R_i + R_j\right)^{4/5}} \quad (6)$$

B. Electron transfer rates

We begin the derivation by considering the rate at which a single grain of radius R_i loses electrons to low-energy states on grains of radius R_j during mixing. Suppose that grains have an unlimited number of acceptor states, and that grain charge does not affect the rate of electron transfer. Then the rate of change of ρ_{Hi} due only to collisions with grains of radius R_j is given by:

$$\left[\frac{d}{dt}\left(4\pi R_i^2 \rho_{Hi}\right)\right]_j = -\omega_{ij} f_H \rho_{Hi} A_{ij} \tag{7}$$

The rate at which ρ_{Hi} changes on this grain due to all collisions is therefore an exponential decay function, given by the integral of Equation 7 over all grain sizes and expanded using the definitions given in the previous sections:

$$\frac{d\rho_{Hi}}{dt} = -\alpha_i \rho_{Hi} \tag{8}$$

$$\alpha_i = \frac{v_r n_0 f_H}{4R_i^2 V_C} \int_0^\infty A_{ik}\left(R_i + R_k\right)^2 g\left(R_k\right) dR_k \tag{9}$$

We can also define the fraction f_{ij} of electrons being transferred to grains of radius R_j, compared to all transferred electrons, as follows:

$$f_{ij} = \frac{\left[d\rho_{Hi}/dt\right]_j}{d\rho_{Hi}/dt} = \frac{A_{ij}\left(R_i + R_j\right)^2 g\left(R_j\right) dR_j}{\int_0^\infty A_{ik}\left(R_i + Rk\right)^2 g\left(R_k\right) dR_k} \tag{10}$$

Note that this fraction has no time dependence; the grain size R_i and size distribution $g(R)$ are the only determining factors. Equations 7 and 10 can also be used to calculate the rate at which our test grain of radius R_i receives electrons during collisions. Starting with Equation 7 (for a single grain of radius R_j this time), we can multiply by n_j and divide by n_i to change this quantity into the rate at which *all* grains of radius R_j lose electrons to our *single* test grain of radius R_i, so that the rate at which our test grain receives (now low-energy) electrons is given by:

$$\frac{d\rho_{Li}}{dt} = -\int_0^\infty \frac{n_j}{n_i}\left[\frac{d\rho_{Hj}}{dt}\right]_i = \int_0^\infty \frac{n_j}{n_i} f_{ji}\alpha_j \rho_{Hj} \tag{11}$$

The overall rate of change of the net charge is given by the sum of Equations 8 and 11:

$$\frac{dQ_i}{dt} = -4e\pi R_i^2\left(\frac{d\rho_{Hi}}{dt} + \frac{d\rho_{Li}}{dt}\right) \tag{12}$$

Integrating this expression, the net charge after all high-energy electrons have been transferred is defined by:

$$Q_i = 4e\pi\rho_0\left(R_i^2 - \int_0^\infty \left[\frac{R_j^2 A_{ij}\left(R_i + R_j\right)^2 g\left(R_j\right)}{\int_0^\infty A_{jk}\left(R_j + R_k\right)^2 g\left(R_k\right)dR_k}\right]dR_j\right) \tag{13}$$

III. Discussion

A. Numerical solutions for Gaussian distribution

Lacks and Levandovsky's original model considered only a finite number of discrete grain radii. However, a far more realistic distribution when the mixture is composed primarily of specific sizes is a sum of normal distributions. While even this may not be sufficient to properly model the size distribution found in most naturally-occurring granular mixtures, it is nonetheless an instructive example in the differences and similarities between our continuous model and the discrete model. We will consider a granular mixture composed of a sum of normal distributions centered on two primary sizes R_1 and R_2, given below:

$$g(R) = k_1 e^{-a_1\left(R-R_1\right)^2} + k_2 e^{-a_2\left(R-R_2\right)^2} \tag{14}$$

We will also specify our convention that $R_2 < R_1$ and define $k = k_2 / k_1$ for the sake of consistency. Here k_i is a factor determining the height of the Gaussian peak corresponding to the distribution of grains near size R_i, so that k is the height of the R_2 peak relative to that of R_1. The coefficients a_1 and a_2 in the exponents are related to the standard deviation of the distributions, a measure of the width of the peaks. Each of these properties can be calculated from the experimentally measured size distribution of a sample of the mixture in question.

Consider now the case for which R_1 = 100μm, R_2 = 50μm, $a_1 = a_2$ = 0.005, and k = 4. The size distribution is shown in Fig. 2a. We can calculate the charge distribution for two cases: the equal contact area assumption made by Lacks and Levandovsky's model, and the size-dependent contact area model using the definition for A_{ij} described above. The final charge distribution is given in Fig. 2b. Note that the equal contact area assumption produces a parabolic charge distribution, in which smaller grain sizes acquire an average negative charge while larger grains become more positively charged. On the other hand, the charge distribution for the size-dependent contact area model includes an additional peak near the small end of the grain size distribution. This means that the smallest grains actually acquire a positive charge, while many large grains are also negatively charged. Notably, while very small grains are predicted to always acquire a positive charge in this model, the charge on the two primary sizes often continue to follow the expected polarity trend.

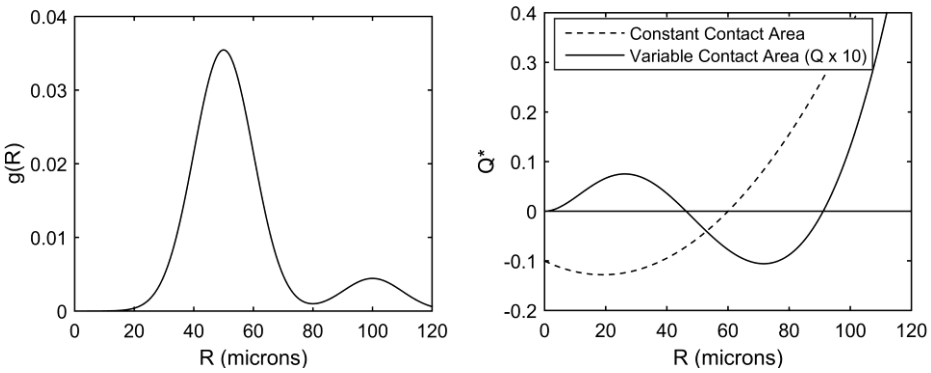

Fig. 2. Non-dimensional charge distribution $Q^* = Q(R) / 4e\pi\rho_0 R_1^2$ for a specified size distribution function. (a) Normalized size distribution function $g(R)$ in the form of Equation 14, with $k_2 / k_1 = 8$, $a_1 = a_2 = 0.005$, $R_1 = 100$ μm, $R_2 = 50$ μm. (b) Charge distribution function corresponding to size distribution in (a) (solid line, magnified x10). For comparison, the distribution using A_{ij} = constant is overlayed (dashed line). Note the large difference in magnitude, and the additional peak in the distribution for our model at low values of R.

B. Comparison to bi-disperse model

Most existing models used today for classifying the behavior of laboratory mixtures employ a discrete size distribution, typically of only two primary grain radii, which we will again call R_1 and R_2. This size distribution can be represented by a sum of two Dirac delta functions $\delta_i = \delta(R-R_i)$, which can be thought of as infinitely narrow normal distributions such that only two grain sizes are represented:

$$g(R) = \frac{k_1\delta_1 + k_2\delta_2}{k_1 + k_2} \tag{15}$$

The total mass m_i of all grains of a single size species can be given by the following expression, where ρ_M is the mass density of the grains:

$$m_i = \frac{4\pi\rho_M}{3(k_1 + k_2)} k_i R_i^3 \tag{16}$$

We can define a set of non-dimensional constants $d = R_2 / R_1 < 1$, $s = (1+d)^2 / 4$, $m = m_2 / m_1 = k\, d^3$, and $r = r_{12} / r_{11} = r_{12} / r_{22}$, which will greatly simplify our analysis. Using Equation 13, we can solve the integrals analytically for the distribution in Equation 15 to obtain the following expressions for the charge in a discrete-sized mixture:

$$Q_{1,discrete} = 4e\pi\rho_0 msrR_1^2 \frac{md - msr - d^2 + dsr}{(d^2 + msr)(dsr + md)} \tag{17}$$

$$Q_{2,discrete} = 4e\pi\rho_0 srd^2 R_1^2 \frac{msr - md + d^2 - dsr}{\left(d^2 + msr\right)\left(m + sr\right)} \tag{18}$$

C. Polarity reversal

Recall that each of the non-dimensional terms *d*, *s*, *m*, and *r* is positive for all sizes R_1 and R_2. Therefore, in Equations 17 and 18, while the denominator is necessarily always positive, the negative terms in the numerator make the signs of Q_1 and Q_2 ambiguous. In previous models, the larger grain size in a bi-disperse mixture always acquires a positive charge, a prediction supported by experimental data; however, these models did not include an area dependence. For our model, we will explore the sign of the numerator of the fraction in Equation 17:

$$sign\left[Q_{1,discrete}\right] = sign\left[\left(m - d\right)\left(d - sr\right)\right] \tag{19}$$

If we recall the definitions of *s* and *r*, we can see that the second term in Equation 19 is always positive:

$$d - sr = d\left(1 - \left[\frac{\left(1+d\right)^3}{4\left(1+d^3\right)}\right]^{2/5}\right) \tag{20}$$

The bracketed expression in Equation 20 ranges from ¼ (as *d* approaches 0) to 1 (as *d* approaches 1); therefore, *d-sr* is positive for all values of *d*. Therefore, from Equation 19, the polarity of the charge on grains of size R_1 is entirely determined by the expression *m-d*. Specifically, the larger grains will only acquire the traditionally-predicted positive polarity if the mixture contains a mass fraction of smaller grains larger than the ratio of their radii to that of the larger grains. Unfortunately, experiments to date cannot confirm or refute their prediction, although as previously discussed, the positive polarity is bar far the more commonly observed.

We have already shown that Lacks and Levandovsky's simplification of a single electron transfer per collision is functionally equivalent to the assumption that all contact areas are equivalent. To better understand the influence of the area term on the charge polarity, let us consider an arbitrary contact area ratio $a_{ij} = A_{ij} / A_{11}$. We will make the very basic assumption that collisions between larger grains cannot, on average, have smaller contact areas than collisions between smaller grains, although we will not yet define the exact relationship between these areas. Thus we have $a_{22} < a_{12} \leq 1$. Returning to Equation 17, we find that the expression determining the polarity can now be written as:

$$sign\left[Q_{1,discrete}\right] = sign\left[d\left(-\frac{d^2}{a_{12}} + s\right) + m\left(\frac{a_{22}}{a_{12}} - s\right)\right] \tag{21}$$

If the contact areas are equal, then $a_{22} = a_{12} = 1$ and we obtain the expression originally found by Lacks and Levandovsky:

$$sign\left[Q_{1,discrete}\right] = sign\left[\left(d\left(1+3d\right)+m\left(d+3\right)\right)\left(1-d\right)\right] \qquad (22)$$

Clearly this expression is always positive, as by definition $d < 1$. However, for size-dependent contact areas, we return to Equation 21. As d decreases from 1, if a_{12} decreases faster than d^2 / s, then the first term will be positive for all values of d greater than some critical value. Similarly, the second term will be negative above a different critical value for d if a_{22} decreases faster than $s\, a_{12}$. The relationship between these rates, and the value of m in the mixture, will determine the overall critical value for d at which the polarity reverses. Because $a_{22} = A_{22} / A_{11}$, and we expect the areas to carry some dependence on surface area, it seems likely that a_{22} is of order d^2 and a_{12} is approximately of order d. This suggests that the parentheticals in Equation 21 both go as d-s, suggesting that Q_1 is approximately proportional to m-d. This reaffirms our observation of the polarity reversal derived above.

This phenomenon has not been reported in experiments to date, but the lack of existing experimental evidence could be attributed a number of factors. For constant contact area, the predictions made by the continuous distribution model closely match those of the discrete model (see Fig. 3), so clearly the disagreement comes from the introduction of a contact area dependence. However, experiments on collisions of spheres suggest that the transferred charge is indeed proportional to the contact area [18-20], suggesting that our implementation of the contact area is accurate. Therefore, either small grains have more irregular surfaces that do not behave as we expect, or there is another phenomenon occurring that masks the dependence on contact area. For example, many grain charging experiments are performed in atmosphere; some experiments have shown that charging in vacuum or a neutral gas produces vastly different charge patterns [17], while others have suggested that humidity from the air adsorbed onto grains dramatically changes the magnitude and/or mechanism of charge exchange [8, 23-25]. These possibilities must be explored to determine under which conditions, if any, our model is applicable.

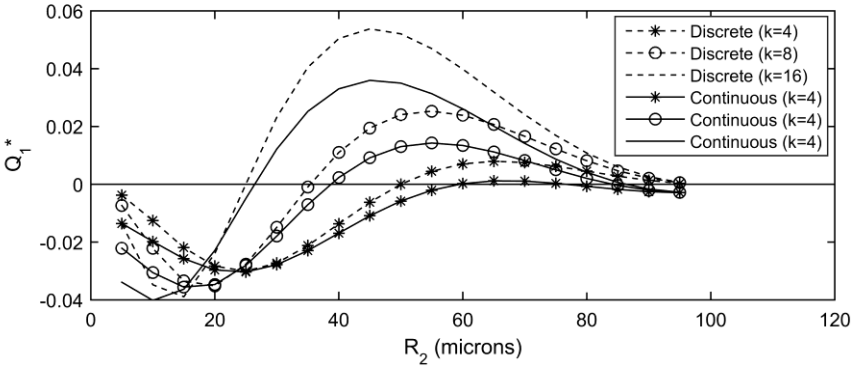

Fig. 3. Non-dimensional charge $Q_1^* = Q_1 / 4e\pi\rho_0 R_1^2$ (from Equation 13) on grains of radius R_1 = 100μm for a size distribution of the form given in Equation 14. Solid lines correspond to the continuous size distribution model, whereas dashed lines correspond to the discrete model. The size distribution has parameters $a_1 = a_2 =$ 0.005, with k and R_2 varied as shown. Note that as R_2 varies relative to R_1, the sign of Q_1 changes. The point at which this reversal occurs is highly dependent on k, which is related to the mass ratio m (see Equation 16). Note that the charge predicted by the continuous distribution is very similar to that predicted by the discrete model, with some variation due to the effect of the nonzero peak width.

It is important to note that, because we are working with a continuous distribution, the concept of "polarity" in the sense used in the discrete model is ambiguous. For example, while the Gaussian distribution used here always produces a positive peak for very small grains regardless of the polarity term, we can observe the polarity reversal by only examining the charge close to the peaks of the distribution. In Fig. 4 we have plotted the charge distribution functions for values $k = 8$ and $d = 0.5$, but with varying peak width. The total mass of each "size species" of grain in the continuous mixture is dependent on the width of the peaks a as well as the relative height k, causing significant variation in polarity even with constant k and d. This confirms that by neglecting the effects of the continuous size distribution on the final charge distribution, past experiments may be obscuring the conditions for a polarity flip. Note that for most real granular mixtures of scientific interest, the size distribution is broader and contains far more than just two discrete sizes; for such mixtures, "polarity" is no longer a well-defined term and will not be considered.

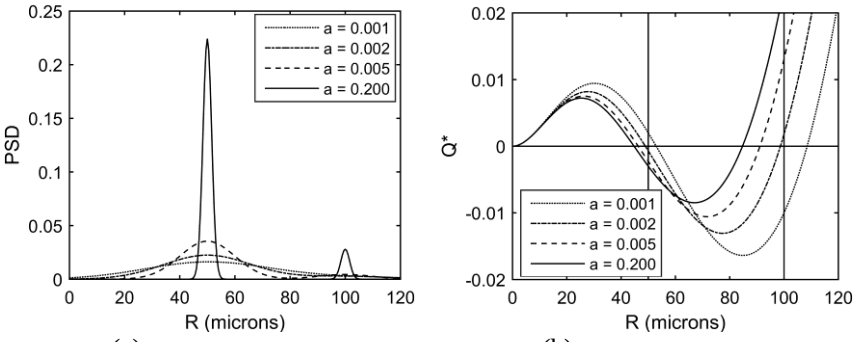

(a) (b)

Fig. 4. Variation of non-dimensional charge distribution $Q^* = Q(R) / 4e\pi\rho_0 R_1^2$ with peak width parameter a. (a) Normalized size distribution function $g(R)$ for various values of a. (b) Charge distribution functions corresponding to size distributions in (a). Vertical lines given as reference at $R = 50$ and $R = 100$, the centers of the peaks in $g(R)$. Note how the grain charge around the peak values changes in polarity with a.

D. Planned experiment

We are currently designing an experimental setup for mixing grains and measuring their individual charges to assess the accuracy of this new model under vacuum conditions. The design is similar to the setup described by Waitukaitis, *et al*, in their 2014 experiment in granular tribocharging [14, 26] (see Fig. 5 for a diagram of their setup). Whereas tribocharging was induced in their experiment under atmospheric conditions, our experimental setup will be entirely housed in vacuum (< 1 mTorr) to eliminate the influence of atmospheric ions and adsorbed humidity. The grains will be fused zirconia silica (69% ZrO_2, 31% SiO_2) from Glenn Mills, Inc., with nominal grain sizes of R_2 = 57.5±5 μm and R_1 = 115±10 μm. By varying the relative masses of each of these sizes species, we can modify the quantity m-d and explore the dependence of charge polarity on these mixture properties.

Grains will be shaken in a small cylindrical container, then poured through a transverse electric field. The interior of the container will be coated with grains to prevent charge exchange with the container walls. The electric field will cause grain trajectories to de-

flect according to charge; these trajectories will be captured by a high-speed camera falling alongside the grains. The camera (Photron FASTCAM Mini UX50) will be capable of measuring grain size to within 5 μm in our design, allowing relatively accurate measurement of the grain radius and mass (from the known material density). The lateral acceleration due to the electric field can then be calculated from the video data, giving a value for the charge-to-mass ratio (and therefore the grain charge, using the calculated mass). By correlating grain size with charge in this way and exploring a variety of mixture properties, we can determine whether or not the predictions in this model are applicable to granular tribocharging under any conditions.

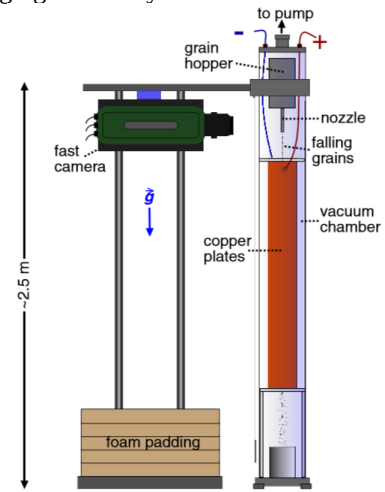

Fig. 5. Experimental setup used in experiments by Waitukaitis, *et al* [14]. Grains are charged in a hopper via fluidization with air, then placed in the vacuum chamber under 3 mTorr conditions. Charged grains are dropped through the E-field between the copper plates, with their trajectories filmed by the camera shown. Our experimental setup (currently in development, but similar in principle) will be housed entirely in vacuum to eliminate potential charge contamination from the atmosphere.

IV. CONCLUSION

In the pursuit of a more realistic model for same-material granular insulator tribocharging, we have built upon the most promising existing models and added additional improvements. By expanding the model to continuous size distributions, we greatly increase the space of real granular mixtures to which tribocharging models can be applied. The predictions made for continuous size distributions are similar to those made for discrete distributions of a similar form, and in the limit where the continuous distribution approaches the latter, the charge predictions converge as well; this suggests that the extension to continuous distributions has not introduced any errors to the model. We have also included room to expand the model to include a dependence on contact area for electron transfer. If this model is correct, it is possible that certain mixture properties may allow for the appearance of a reversal in the usual polarity of charge separation for mixtures of two primary grain sizes. Leading theories on insulator charging suggest that

charging in vacuum or under different humidity conditions may lead to different charging behavior, especially charge separation magnitude and polarity of final charge; controlling these parameters may allow for future testing of this polarity reversal. Alternatively, the deviation in predictions from observed charging behavior may suggest that trapped electrons are not in fact the charge carriers involved in granular insulator tribocharging. Further work will reveal whether these testable predictions are an accurate representation of the charging behavior, and if not, what this means for our current understanding of insulator tribocharging and the trapped electron model in general.

REFERENCES

[1] T. Pahtz, H. Herrmann, and T. Shinbrot, "Why do particle clouds generate electric charges?" *Nature Physics*, vol. 6, pp. 364-368, May 2010.

[2] J. Kok and N. Renno, "Electrostatics in wind-blown sand," *Physical Review Letters*, vol. 100, Jan 2008.

[3] X. Zheng, N. Huang, and Y. Zhou, "Laboratory measurement of electrification of wind-blown sands and simulation of its effect on sand saltation movement," *Journal of Geophysical Research – Atmospheres*, vol. 108, May 2003.

[4] J. Gilbert, S. Lane, R. Sparks, and T. Koyaguchi, "Charge measurements on particle fallout from a volcanic plume," *Nature*, vol. 349, pp. 598-600, Feb 1991.

[5] S. Liang, J. Zhang, and L. Fan, "Electrostatic characteristics of hydrated lime powder during transport," *Industrial & Engineering Chemistry Research*, vol. 35, pp. 2748-2755, Aug 1996.

[6] G. Hendrickson, "Electrostatics and gas-phase fluidized bed polymerization reactor wall sheeting," *Chemical Engineering Science*, vol. 61, pp. 1041-1064, Feb 2006.

[7] D. Saville, M. Al-Adel, and S. Sundaresan, "The effect of static electrification on gas-solid flows in vertical risers," *Industrial & Engineering Chemistry Research*, vol. 41, pp. 6224-6234, Dec 2002.

[8] P. Cartwright, S. Singh, A. G. Bailey, and L. J. Rose, "Electrostatic charging characteristics of polyethylene powder during pneumatic conveying," *IEEE Transactions on Industry Applications*, 1985.

[9] K. M. Forward, D. J. Lacks, and R. M. Sankaran, "Triboelectric charging of lunar regolith simulant," *Journal of Geophysical Research*, vol. 114, no. A10109, Oct 2009.

[10] K. M. Forward, D. J. Lacks, and R. M. Sankaran, "Particle-size dependent bipolar charging of Martian regolith simulant," *Geophysical Research Letters*, vol. 36, no. L13201, Jul 2009.

[11] K. M. Forward, D. J. Lacks, and R. M. Sankaran, "Charge segregation depends on particle size in triboelectrically charged granular materials," *Physical Review Letters*, vol. 102, no. 028001, Jan 2009.

[12] D. J. Lacks, N. Duff, and S. K. Kumar, "Nonequilibrium accumulation of surface species and triboelectric charging in single component particulate systems," *Physical Review Letters*, vol. 100, no. 188305, May 2008.

[13] D. J. Lacks and A. Levandovsky, "Effect of particle size distribution on the polarity of triboelectric charging in granular insulator systems," *Journal of Electrostatics*, vol. 65, pp. 107-112, Jul 2006.

[14] S. R. Waitukaitis, V. Lee, J. M. Pierson, S. L. Forman, and H. M. Jaeger, "Size-dependent same-material tribocharging in insulating grains," *Physical Review Letters*, vol. 112, no. 218001, May 2014.

[15] J. Lowell and W. Truscott, "Triboelectrification of identical insulators: I. An experimental investigation," *Journal of Physics D: Applied Physics*, vol. 19, pp. 1273-1280, 1986.

[16] J. Lowell and W. Truscott, "Triboelectrification of identical insulators: II. Theory and further experiments," *Journal of Physics D: Applied Physics*, vol. 19, pp. 1281-1298, 1986.

[17] T. Shinbrot, T. Komatsu, and Q. Zhao, "Spontaneous tribocharging of similar materials," *Europhysics Letters*, vol. 83, Jul 2008.

[18] T. Matsuyama and H. Yamamoto, "Charge transfer between a polymer particle and a metal plate due to impact," *IEEE Transactions on Industry Applications*, vol. 30, pp. 602-607, 1994

[19] H. Watanabe, A. Samimi, Y. L. Ding, M. Ghadiri, and T. Matsuyama, "Measurement of charge transfer due to single particle impact," *Particle and Particle Systems Characterization*, vol. 23, pp. 133-137, Aug 2006.

[20] S. Matsusaka, M. Ghadiri, and H. Masuda, "Electrification of an elastic sphere by repeated impacts on a metal plate," *Journal of Physics D: Applied Physics*, vol. 33, pp. 2311-2319, 2000.

[21] S. Matsusaka, H. Maruyama, T. Matsuyama, and M. Ghadiri, "Triboelectric charging of powders: a review," *Chemical Engineering Science*, vol. 65, pp. 5781-5807, Jul 2010.
[22] D. Gugan, "Inelastic collision and the Hertz theory of impact," *American Journal of Physics*, vol. 68, no. 920, 2000.
[23] S. Pence, V. Novotny, and A. Diaz, "Effect of surface moisture on contact charge of polymers containing ions," *Langmuir*, vol. 10, pp. 592-596, Feb 1994.
[24] A. Wiles, M. Fialkowski, M. Radowski, G. M. Whitesides, and B. Gryzbowski, "Effects of surface modification and moisture on the rates of charge transfer between metals and organic materials," *Journal of Physical Chemsity B*, vol. 108, pp. 20296-20302, Dec 2004.
[25] L. S. McCarty and G. M. Whitesides, "Electrostatic charging due to separation of ions at interfaces: contact electrification of ionic electrets," *Angewandte Chemie International Edition*, vol. 47, pp. 2188-2207, Mar 2008.
[26] S. R. Waitukaitis and H. M. Jaeger, "In situ granular charge measurement by free-fall videography," *Review of Scientific Instruments*, vol. 84, no. 025104, Feb 2013.